Scope and Limitations of Surface Functional Group Quantification Methods: Exploratory Study with Poly(acrylic acid)–Grafted Micro- and Nanoparticles

10 AUTHORS, INCLUDING:

Andreas Hennig
Jacobs University

53 PUBLICATIONS **1,243** CITATIONS

Christian Würth
Bundesanstalt für Materialforschung und -prü…

29 PUBLICATIONS **462** CITATIONS

Katrin Hoffmann
Bundesanstalt für Materialforschung und -prü…

72 PUBLICATIONS **1,332** CITATIONS

Ute Resch-Genger
Bundesanstalt für Materialforschung und -prü…

179 PUBLICATIONS **5,113** CITATIONS

Scope and Limitations of Surface Functional Group Quantification Methods: Exploratory Study with Poly(acrylic acid)–Grafted Micro- and Nanoparticles

Andreas Hennig,*,[†] Heike Borcherding,[‡] Christian Jaeger,[†] Soheil Hatami,[†] Christian Würth,[†] Angelika Hoffmann,[†] Katrin Hoffmann,[†] Thomas Thiele,[‡] Uwe Schedler,[‡] and Ute Resch-Genger*,[†]

[†]BAM Federal Institute for Materials Research and Testing, Richard-Willstätter-Strasse 11, D-12489 Berlin, Germany
[‡]PolyAn GmbH, Rudolf-Baschant-Strasse 2, D-13086 Berlin, Germany

S *Supporting Information*

ABSTRACT: The amount of grafted poly(acrylic acid) on poly(methyl methacrylate) micro- and nanoparticles was quantified by conductometry, ^{13}C solid-state NMR, fluorophore labeling, a supramolecular assay based on high-affinity binding of cucurbit[7]uril, and two colorimetric assays based on toluidine blue and nickel complexation by pyrocatechol violet. The methods were thoroughly validated and compared with respect to reproducibility, sensitivity, and ease of use. The results demonstrate that only a small but constant fraction of the surface functional groups is accessible to covalent surface derivatization independently of the total number of surface functional groups, and different contributing factors are discussed that determine the number of probe molecules which can be bound to the polymer surface. The fluorophore labeling approach was modified to exclude artifacts due to fluorescence quenching, but absolute quantum yield measurements still indicate a major uncertainty in routine fluorescence-based surface group quantifications, which is directly relevant for biochemical assays and medical diagnostics. Comparison with results from protein labeling with streptavidin suggests a porous network of poly(acrylic acid) chains on the particle surface, which allows diffusion of small molecules (cutoff between 1.6 and 6.5 nm) into the network.

■ INTRODUCTION

Micro- and nanoparticles are of current interest for a range of applications in materials sciences, life sciences, and medicine, including, for example, DNA sequencing, fluorescence-based assays, sensors, in vivo imaging, drug delivery, and optoelectronic devices.[1−16] The key to better understand and control their materials properties and interactions with other molecules lies in the precise knowledge of the number, chemical nature, and spatial distribution of their surface functional groups.[17,18] Up-to-date methods for quantifying the number of surface functional groups include, for example, attenuated total reflectance Fourier transform infrared spectroscopy (ATR-FTIR), X-ray photoelectron spectroscopy (XPS), solid-state NMR, or isothermal titration calorimetry.[19−21] However, for determination of acidic or basic surface functional groups, potentiometry and conductometry are still among the most widely used methods, because they are relatively straightforward to implement and do not require highly sophisticated and specialized instrumentation.[22−25] As an alternative, colorimetric or fluorometric assays have been developed, which are faster and more sensitive but may suffer from certain artifacts if not properly validated.[26−33]

While these label-free methods report on the *total* number of surface functional groups, it is also of high interest how many application-relevant molecules such as peptides, proteins, antibodies, or DNA can be principally conjugated to the particle surface. This quantity can differ from the *total* number of surface functional groups and has been referred to as the number of *accessible* (or available) functional groups. To determine the number of accessible functional groups, a specific detection label, for example, a fluorescent probe, radiotracer, or a heteroatom-containing XPS label, is covalently attached and quantified.[33−43]

Owing to the vast number of different methods and techniques available for quantification of surface functional groups, a systematic comparison among different methods is highly desirable to elucidate the advantages and disadvantages of each method in terms of usability, application scope, and operational reliability. Moreover, it is unclear whether and to which extent the numbers of total and accessible functional groups are interrelated and how the size of the detection label influences the maximal achievable coupling yields. This would afford a rough estimate of how much of a molecule can be maximally coupled to the particle surface, which would consequently allow saving precious material. A thorough and reliable quantification of surface functional groups is also directly relevant to avoid systematic errors in biochemical assays and for standardization in medical diagnostics.

Herein, we report a study, which includes conductometry, solid-state NMR, two colorimetric assays, fluorophore labeling, and an assay based on supramolecular host−guest interactions, to determine the number of total and accessible functional groups on poly(methyl methacrylate) (PMMA) particles (mean diameter from 100 nm to 11 μm) with a covalently linked layer of varying amounts (21−7000 μmol g^{-1}, P01−P22, see Table S-1 in Supporting Information) of grafted poly-(acrylic acid) (PAA). The main criteria for method choice were ease of use with common laboratory equipment or suitability for validation of results obtained by the other methods reported herein. Conductometry and adsorption/desorption-based colorimetric toluidine blue (TB) assay are relatively well established.[25,30−32] The colorimetric assay based on complex formation between Ni^{2+} and pyrocatechol violet (PV) and the supramolecular assay based on host−guest complexation by cucurbit[7]uril (CB7) were recently communicated by us,[26,34] and the solid-state ^{13}C NMR as well as a strongly modified fluorophore labeling approach in conjunction with absolute quantum yield measurements with a custom-made calibrated integrating sphere setup[44−46] are reported herein for the first time. Topics addressed include shortcomings and limitations of each method, which provides guidelines for chemists in choosing a suitable method for surface group quantifications, how our results relate to biologically and medicinally relevant applications, and how the three-dimensional spatial arrangement of surface functional groups may affect the outcome of these experiments, a topic which is so far clearly underexplored.

■ RESULTS

Conductometry and Solid-State NMR. Conductometric titrations for quantifying the total number of acidic and basic surface functional groups are frequently used because of their apparent simplicity. Therein, complete protonation or deprotonation of all surface functional groups is commonly presumed,[22,24] which may, however, occasionally require drastically elongated equilibration times to allow diffusion of titrant ions into the polymer network and avoid a systematic underestimate.[23,25] In our case, base-into-acid titrations in the presence of 0.3 mM KBr as a neutral salt[22] were performed to determine the total number of COOH groups on the particle surface, and a stable conductivity value was reached after 5−10 min. The results indicated PAA surface concentrations in the range of 21−7000 μmol g^{-1} (see Table S-1, Supporting Information, for details) and were determined with the intention to serve as benchmark values in this report, when compared with results from the other methods.

To really ensure that no systematic underestimate by incomplete surface deprotonation occurs, we additionally decided to validate the amount of surface COOH groups by an independent method. A particular challenge of the presently investigated particle system lies in the chemical similarity of the PMMA particles and the grafted PAA layer, which leads to a significant signal overlap in most conceivable spectroscopic methods. We thus resorted to solid-state ^{13}C NMR, in which we expected a selective and quantitative signal enhancement when PAA is grafted onto the PMMA particles.[19] This signal enhancement was readily detectable for polymer particles with the highest PAA (P22, see Table S-1 and Figure S-2, Supporting Information) and gave a surface COOH concentration of 5600 ± 600 μmol/g, which is in reasonable agreement with 7000 ± 800 μmol/g as determined by conductometry and unambiguously eliminates the possibility of incomplete surface group deprotonation. However, accurate quantification by NMR becomes much more involved for less than approximately 20% of signal enhancement, which frequently hampers the use of NMR in quantifying trace amounts in component mixtures.[47] The challenge here is discrimination between the small number of surface functional groups and the bulk material of the particle in conjunction with the strong chemical resemblance of both materials. For example, a 100 nm particle covered with a monolayer of surface carboxy groups (ca. 0.5 nmol/cm^2)[24] has a molar surface-to-particle ratio of just about 2 mol %, which renders conventional NMR determination futile. This discrepancy led us to the idea to graft ^{13}C-enriched acrylic acid (99% ^{13}COOH) onto a PMMA core with natural ^{13}C abundance (1.1% ^{13}COOH) and thereby obtain a selective signal enhancement from the grafted COOH surface groups by 2 orders of magnitude. In the present case, the ratio of carboxylic acid/ester to methyl groups is 1:1 for unmodified PMMA particles, and grafting of ^{13}COOH-enriched PAA led to a sufficiently large increase in the signal from the carboxylic acid/ester groups (Figure S-3, Supporting Information), which could be easily quantified. Thereby, the remaining NMR signals served as a convenient internal standard. By this method (see Supporting Information for details) we determined a PAA surface concentration of 36 ± 4 μmol/g (P09), which is in excellent agreement with 40 ± 4 μmol/g from conductometry. This agreement mutually confirmed the precision and trueness of both methods and unequivocally demonstrated that the surface COOH groups of polymer particles with both very low and very high amounts of grafted PAA can be completely deprotonated. Since the time to reach the protonation/deprotonation equilibrium is expected to be dependent on specific parameters of the system under study, e.g., thickness and morphology of the surface layer, it can be concluded that a systematic variation is also very unlikely for particles containing intermediate amounts of surface COOH groups.

Colorimetric Assays. Colorimetric assays present a faster and more sensitive alternative to conductometric titrations. For example, adsorption/desorption-based dye assays have been developed in which a dye of complementary charge is adsorbed onto a particle surface.[28−33] After extensive washing, the dye is desorbed from the particle surface and the dye concentration of the colored desorption solution is determined by absorption or fluorescence spectroscopy to afford a measure for the number of surface functional groups. The most popular adsorption/desorption-based dye assay for quantification of surface COOH groups is based on toluidine blue O (TB),[28−31] which prompted us to include the TB assay in this work. We followed the classical method previously reported by Sano et al.[27,31] and found a linear correlation ($R > 0.93$, 22 samples) between the number of COOH groups determined by the TB assay and by conductometry. However, by assuming a one-to-one binding stoichiometry between TB and surface COOH groups as originally proposed,[30−32] markedly lower amounts of surface COOH groups would result. Linear fitting rather suggested that 3.4 ± 0.2 COOH groups bind one TB molecule. By using this stoichiometry factor, Figure 1a was obtained, and the respective values, which compare relatively well with the results from conductometry, are included in Table S-1, Supporting Information.

As a potential alternative to the TB assay, we recently introduced a method which exploits that Ni^{2+} is efficiently bound by PAA-modified polymer particles, allowing extraction
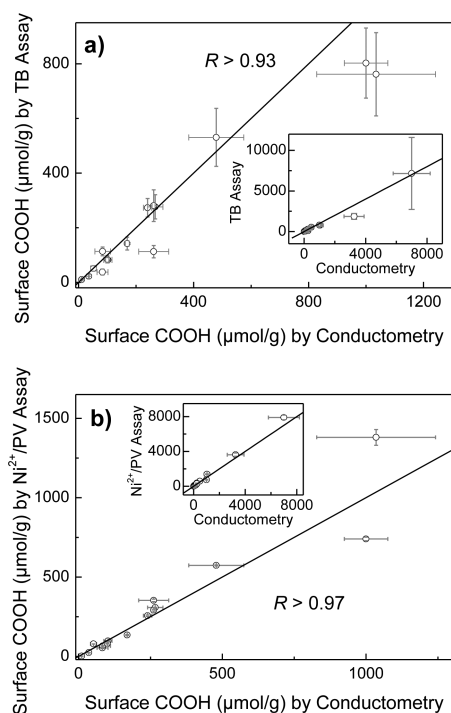
Figure 1. Correlations between the number of surface carboxy groups on PMMA micro- and nanoparticles (diameter = 0.1−11 μm) determined by conductometry and (a) TB assay and (b) Ni^{2+}/PV assay. Error bars indicate the standard deviation ($n \geq 3$). Stoichiometry factors of 3.4 and 2.65 for the TB and Ni^{2+}/PV assay were applied to account for the different numbers of COOH groups per TB or Ni^{2+}. Accordingly, the results should coincide with an ideal one-to-one correlation (solid lines). (Inset) Whole range of particles investigated (10−7000 μmol/g surface PAA).

of Ni^{2+} in a single centrifugation step.[26] Remaining Ni^{2+} in the supernatant is subsequently quantified by the transition metal ion indicator pyrocatechol violet (PV).[48] A linear correlation between the amount of extracted Ni^{2+} and the number of surface COOH groups indicated that 2.65 ± 0.03 COOH groups are required to extract one Ni^{2+} ion. Herein, additional surface group quantifications are included and backed up by the previously communicated results to expand our data set (see Table S-1, Supporting Information). The excellent reproducibility of the Ni^{2+}/PV assay was as well maintained as the linear relationship with the results from conductometry (Figure 1b).

Fluorophore Labeling. Although attractive owing to its extremely high sensitivity, fluorophore labeling has rarely been applied to a rigorous quantitative analysis of surface functional groups on particles[41] but was more restricted to planar substrates.[33,40,42,49−51] The materials properties of our particles precluded the use of organic solvent during fluorophore labeling, which would lead to particle swelling and nonselective incorporation of fluorescent dyes or at worst dissolution of the particle. Since reactive fluorophores for COOH group labeling in water are principally nonexistent, we used 1-ethyl-3-(3-dimethylaminopropyl) carbodiimide (EDC) for activation of the surface COOH groups.[52,53] As fluorescent dye, we selected a 1,6-diaminohexane derivative of fluorescein-5-isothiocyanate (FL-A), which was synthesized by a slightly modified literature procedure (see Supporting Information).[54]

During our initial efforts to develop a labeling protocol we noted that different particle preparations had similar fluorescence intensities despite a clearly different color

intensity. This was attributed to self-quenching of spatially adjacent fluorophores at high local dye concentrations on the particle surface. Furthermore, a stronger tendency for particle aggregation was observed after FL-A labeling, presumably owing to the high concentration of large hydrophobic aromatic groups on the particle surface. To bypass these problems we devised a surface dilution strategy in which mixtures of FL-A (0−30 mol %) and $H_2N−CH_2(OCH_2)_3−CO_2tBu$ were used during the coupling reaction. Therein, $H_2N−CH_2(OCH_2)_3−CO_2tBu$ spatially separates FL-A molecules from each other on the surface and thus minimizes the probability of self-quenching. Additionally, the *tert*-butyl ester group from $H_2N−CH_2(OCH_2)_3−CO_2tBu$ can be subsequently removed by incubation with an acid, which restores a negatively charged surface and reduces the propensity for particle aggregation.

Successful implementation of this strategy was confirmed by confocal laser scanning microscopy (CLSM) and fluorescence spectroscopy (Figure 2). CLSM images immediately revealed
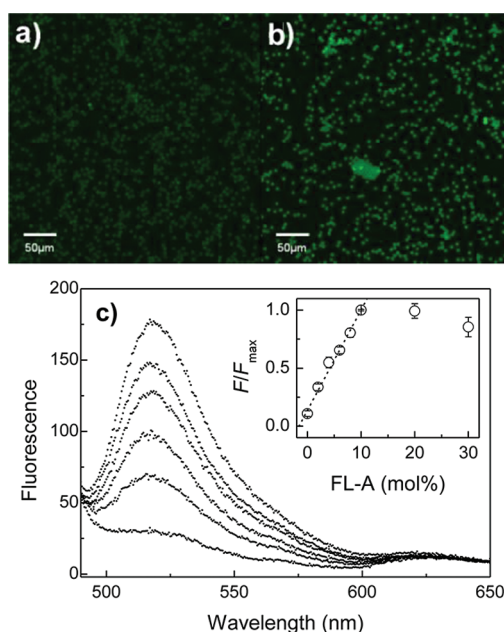
Figure 2. Fluorescence microscopic (top) and spectroscopic (bottom) analysis of PMMA particles P01 after labeling with a mixture of FL-A and $H_2N−CH_2(OCH_2)_3−CO_2tBu$. CLSM images ($\lambda_{exc}$ = 488 nm, λ_{em} = 500−600 nm) with (a) 2% FL-A and (b) 30% FL-A indicate the reduced propensity for particle aggregation with reduced mol % FL-A. (c) Steady-state fluorescence spectra (λ_{exc} = 475 nm, 0.74 mg/mL P01) with increasing percentage of FL-A (0, 2, 4, 6, 8, and 10 mol %) in 0.1 M borate buffer, pH 9.0. (Inset) Plot of the fluorescence intensity (λ_{obs} = 517 nm) normalized to the maximum fluorescence (F/F_{max}) versus mol % of FL-A. Broken line was obtained by linear regression ($R > 0.99$) of the initial part (0−10% FL-A).

that a higher mol % of FL-A during particle labeling leads to higher fluorescence intensities but also to an increased propensity for formation of particle aggregates (Figure 2a and 2b). Importantly, control experiments in which EDC was omitted gave nonfluorescent particles, which indicated covalent tethering of FL-A to the particle and excluded the possibility of nonspecific surface adsorption. The dependence of the fluorescence intensity on the mol % of FL-A was investigated in more detail by measuring fluorescence spectra of particles with varying mol % of FL-A (Figure 2c) at constant particle concentrations. For almost all labeled particles (see Supporting

Information) the fluorescence intensity initially increased linearly and showed downward curvature at higher mol %, demonstrating that fluorescence self-quenching of spatially adjacent fluorophores can be successfully suppressed at low FL-A mol %. These results were also confirmed for selected particles by measuring fluorescence spectra with our CLSM setup (see Figure S-7, Supporting Information).

Presuming a similar reactivity of FL-A and H$_2$N−CH$_2$(OCH$_2$)$_3$−CO$_2$tBu and low absorbances, the total concentration of derivatized functional groups s_p can be calculated according to eq 1 (see Supporting Information)

$$s_p = \frac{100 m_p \Phi_f \varepsilon_f}{m_f \Phi_p \varepsilon_p w_p} \qquad (1)$$

in which m_f is the slope of a calibration curve (measured with 5(6)-carboxyfluorescein (CF)), m_p the slope of the initial linear fluorescence increase in the FL-A mol % plot, Φ_f the quantum yield of CF, ε_f the molar absorption coefficient of CF at the excitation wavelength, Φ_p the (average) quantum yield of FL-A on the particle surface in the absence of quenching, ε_p the molar absorption coefficient of FL-A on the particle surface at the excitation wavelength, and w_p the mass concentration of particles. However, application of eq 1 will additionally require knowledge of the ratio of $\varepsilon_f/\varepsilon_p$ and Φ_f/Φ_p.

To account for potentially different ε_f and ε_p, absorption spectra of CF, FL-A in solution and FL-A on particles were measured, corrected by a simple fit for the contributions of particle scattering, and normalized to equal areas under the $\pi-\pi^*$ absorption band around 490 nm (Figure 3).[55−60] These
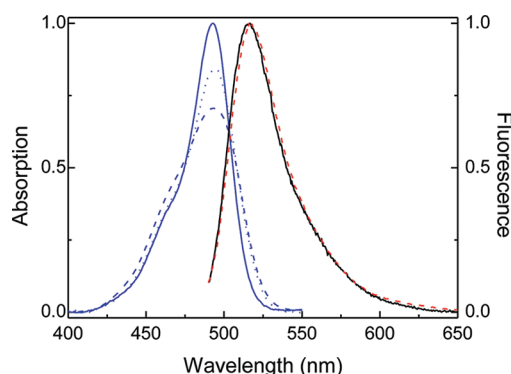
Figure 3. Absorption spectra (blue) of CF (solid line), 6% FL-A (dotted line) and 20% FL-A (dashed line) on P21, and fluorescence spectra (λ_{exc} = 475 nm) of CF (solid black line) and 2−30% (background-subtracted, normalized and averaged) FL-A on P21 (dashed red line) in 0.1 M borate buffer, pH 9.0. The absorption spectra were normalized to equal areas under the absorption band.

spectra showed a broadening and splitting of the absorption band into two bands at higher and lower energy with increasing mol % of FL-A, indicating formation of nonfluorescent H-type dimers,[61] which is consistent with the implications made above from fluorescence measurements. More important, these spectra revealed an intersection at ca. 475 nm, which indicates that $\varepsilon_f/\varepsilon_p$ can be approximated as 1, when this wavelength is selected for excitation (see Supporting Information for details).

In contrast, fluorescence of xanthene dyes such as fluoresceins is much more sensitive to environmental effects than absorption. Although the position and shape of the fluorescence bands of CF and FL-A (regardless of its mol %)

on the particles are essentially the same (see Figure 3), this does not imply identical fluorescence quantum yields of FL-A on the particle surface and in solution. Consequently, absolute fluorescence quantum yields of CF, FL-A, and the labeled particles were determined in 0.1 M borate buffer pH 9.0 with a calibrated integrating sphere spectrometer.[44−46] Note that fluorescence quantum yields of fluorescent particles were until recently[46,62,63] not determined absolutely but only relatively[64] or as powders in dried form.[65−67] Most importantly, this essential fluorometric key parameter has so far not been considered in fluorometric surface group quantifications. With this method, a quantum yield of 0.86 ± 0.02 was obtained for CF, which is a commercially available mixture of the 5- and 6-isomer. This value is in excellent agreement with literature values of 0.834 and 0.915 for the 5- and 6-isomer, respectively.[68] As expected, the fluorescence quantum yield of FL-A on the particle surface decreased with increasing mol % FL-A owing to an increased probability of nonfluorescent dimer formation (see Figure S-8, Supporting Information). To ascertain the theoretical quantum yield in the absence of self-quenching effects, an extrapolation to 0% FL-A was performed and the results are summarized in Table 1. Surprisingly, we found that the quantum yield on particles is not only different from the solution value (0.57 ± 0.02) but also varies markedly from 0.14 to 0.41 depending on the total number of surface COOH groups. In our case, this would lead to an underestimate of the number of surface functional groups in the range of ca. 25−70%, even when self-quenching effects are thoroughly excluded. This should be accounted for even though the fluorophore approach itself is very reproducible (variation coefficient of 5%, six replicates). Nonetheless, when determining the number of accessible surface functional groups according to eq 1 we found a fair linear correlation with the total number of functional groups ($R > 0.93$, see Figure 4). On average, the coupling yield was around 3.8 ± 1.7% of the total number of functional groups (see Table 1), which is in reasonable agreement with results from the CB7 assay.[34]

Supramolecular CB7 Assay. As an elegant alternative to fluorophore labeling, we recently introduced a supramolecular method to determine the number of accessible surface functional groups.[34] In brief, the CB7 assay works such that the polymer particles are functionalized with N-(adamantane methyl)-butane-1,4-diamine after activation by EDC. The highly specific and very strong binding of adamantane methylamines to the macrocyclic supramolecular host molecule CB7 ($K_a > 10^{14}$ M^{-1}) has been recently established[34,69,70] and serves here to capture CB7 from solution to the particle surface. Centrifugation separates particle-bound CB7 from remaining CB7 in solution. The latter is subsequently quantified by addition of the fluorescent dye acridine orange,[71−73] and the difference between added and remaining CB7 affords the amount of CB7 bound to the surface. This is reminiscent of the Ni^{2+}/PV assay, because the spectroscopic measurement is performed in the absence of particles and thus in homogeneous solution. The results of the CB7 assay are summarized in Table 1. On average, 5.2 ± 1.5% of all surface functional groups are accessible by the CB7 assay, which is consistent with the results from fluorophore labeling. The standard deviation is slightly lower, and the correlation between the total number of functional groups and the accessible number of functional groups as determined by the CB7 is much better ($R > 0.99$, see Figure 5). Moreover, the excellent reproducibility of the CB7 assay is reflected in a variation coefficient of 6% (six replicates).
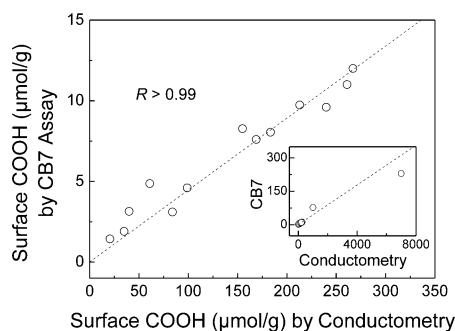
Table 1. Determination of Accessible Functional Groups by Fluorophore Labeling and a CB7-Based Supramolecular Receptor-Ligand Binding Assay

particle batch	diameter (μm)	conductometry[a] s (μmol/g)	fluorophore labeling[b] Φ_p	μmol/g	yield (%)	nmol/cm²	CB7 assay[c] μmol/g	yield (%)	nmol/cm²
P08	0.1	183[d]	0.29 ± 0.02	3.5	1.9	0.015	8.1	4.4	0.028
P09	0.11	40	0.24 ± 0.03	0.48	1.2	0.0034	3.1	7.8	0.014
P10	6	21	0.14 ± 0.02	0.86	4.0	0.16	1.4	6.7	0.33
P11	6	35	0.32 ± 0.03	1.1	3.2	0.36	1.9	5.4	0.46
P12	6	61	0.19 ± 0.02	3.2	5.3	0.82	4.9	8.0	1.2
P13	6	84	0.33 ± 0.02	2.2	2.6	0.61	3.1	3.7	0.74
P14	6	99	0.32 ± 0.04	3.8	3.9	1.0	4.6	4.6	1.1
P15	6	155	0.24 ± 0.03	6.7	4.3	1.9	8.3	5.4	2.0
P16	6	170	0.30 ± 0.03	8.0	4.8	1.8	7.6	4.5	1.8
P17	6	213	0.24 ± 0.03	8.7	4.1	2.4	9.7	4.6	2.3
P18	6	240	0.29 ± 0.01	10	4.3	2.7	9.6	4.0	2.3
P19	6	261	0.26 ± 0.01	19	7.2	4.2	11	4.2	2.6
P20	6	267	0.31 ± 0.02	8.0	3.0	2.3	12	4.5	2.9
P21	6	946	0.41 ± 0.02	21	2.2	5.4	77	7.7	18
P22	6	7000	0.36 ± 0.03	9.2[e]	0.13[e]	2.3[e]	230	3.3	55

[a]Error 9%. [b]Error 5%, determined for P15 (six replicates). [c]Error 6%, values taken from ref 34 except for P08–P10, P12, P15, and P17. [d]As given by supplier, polystyrene core. [e]Derivatization not complete (see Supporting Information).
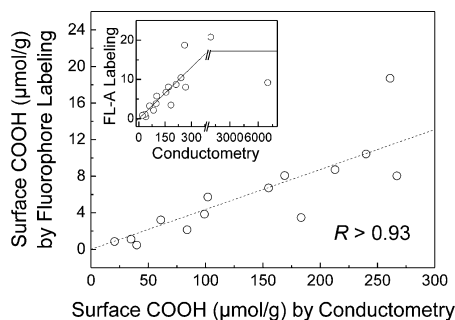
Figure 4. Correlation between the total number of surface functional groups determined by conductometry and the number of accessible functional groups by fluorophore labeling with FL-A.
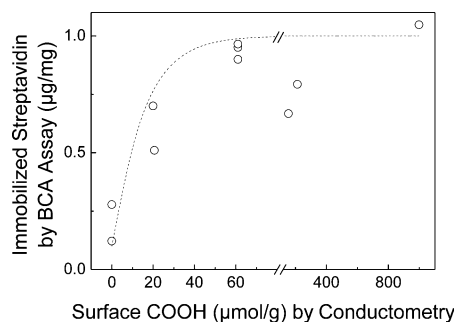

Figure 5. Correlation between the total number of surface functional groups determined by conductometry and the number of accessible functional groups by the CB7 assay.

Biolabeling. As a pertinent example for conjugating an application-relevant molecule to the particle surface we selected streptavidin, which is a well-defined and frequently used model system for biomolecule conjugation.[18,41,74,75] Furthermore, the specific and high-affinity binding of biotin by streptavidin allows a convenient, noncovalent, and reversible functionalization of streptavidin-coated particles, which is directly relevant for numerous applications. Conjugation of streptavidin was carried out according to standard procedures by activating the COOH groups with EDC, converting them into the *N*-hydroxysuccinimide (NHS) ester, and transferring the activated particles into the conjugation buffer with streptavidin.[52,53] This two-step procedure prevents potential activation of acidic residues of streptavidin by EDC and cross-linking by amide formation with basic residues of another streptavidin protein.[52] Subsequently, surface-bound streptavidin was quantified by the bicinchoninic acid assay (BCA assay).[76]

The correlation between surface-bound streptavidin and the conductometrically determined total concentration of surface COOH groups is shown in Figure 6. Similar to the results from

Figure 6. Correlation between the amount of protein (μg/mg) conjugated to the particle surface and the total number of surface COOH groups determined by conductometry. Broken line was obtained by tentatively fitting the data to an exponential function and is included to guide the eye.

fluorophore labeling and the CB7 assay, an approximately linear relationship between surface-bound streptavidin and the number of surface functional groups was found, which, however, reached a plateau region at ca. 1 μg/mg particles. This refers to a surface density of 4 pmol/cm² streptavidin, which matches the value expected for a streptavidin monolayer.[77] This striking difference in the maximally achievable labeling density between a protein and a small molecule (FL-A/CB7) allows properties of the surface polymer morphology to be inferred (see Discussion).

■ DISCUSSION

Reproducibility, Sensitivity, and Performance. On the basis of the combined results presented herein we now compare and discuss the methods with respect to reproducibility, sensitivity, and ease of use according to our hands-on experience. An overview of the sensitivity and reproducibility is given in Table 2, and details on how the sensitivity was assessed

Table 2. Sensitivity and Precision of Different Methods

method	sensitivity[a] (nmol)	precision[b]
conductometry	1000	9%
^{13}C NMR	~10[5]	ca. 10%
TB assay	15[c]	14%
Ni^{2+}/PV assay	50	5%
fluorophore labeling	50[c]	5%
CB7 assay	20[c]	6%

[a]See Supporting Information for details on how the sensitivity was approximately assessed. [b]Expressed as coefficient of variation (see Supporting Information for details on NMR, $n \geq 3$ for conductometry, $n \geq 6$ other methods). [c]Significantly larger amounts may be required to avoid problems related to handling small amounts of particles (<5 mg).

can be found in the Supporting Information. Conductometry and solid-state NMR are both fairly reproducible, but both methods require relatively large amounts of material owing to their rather limited sensitivity (see Table 2). Furthermore, both methods are overall tedious and time consuming. For example, sensitive conductometric titrations require deionized and decarbonated water (<10^{-6} μS/cm) as well as standard solutions with known titer, and quantitative solid-state ^{13}C NMR requires optimized relaxation times between individual pulses and sophisticated instrumentation not available to the common laboratory. Furthermore, for low amounts of surface functional groups this method is unsuitable as it requires grafting of an isotope-enriched surface layer. Hence, this approach is rather suited as a reference method for validation of more simple methods as used herein than as a generally applicable routine measurement.

To overcome the limited sensitivity of conductometry and NMR, colorimetric dye assays have been introduced, among which the widely used TB assay,[27−31] and the recently reported Ni^{2+}/PV assay were included in this study. As expected, both colorimetric assays are ca. 20−60 times more sensitive than conductometric titrations (Table 2). The TB assay is theoretically slightly more sensitive, but it suffers from its poor reproducibility and laborious protocol. The reproducibility can be improved by including a final particle drying and weighing step to account for partial material losses during excessive washing cycles of the strongly colored TB solution. This reduced the variation coefficient to an acceptable 14%, but this precision is still inferior compared to all other methods investigated herein. Furthermore, it sacrifices sensitivity because a sufficient amount of particles (ca. 5 mg) is required for the ultimate weighing step. In contrast, the Ni^{2+}/PV assay allows measuring the supernatant after a single centrifugation step. This dramatically facilitates sample preparation, because it addresses the need for repeated washing cycles and eliminates the possibility of material losses, which is reflected in a variation coefficient of 5%.

Overall, each method for determining the total number of surface COOH groups has its particular application area. The main advantage of conductometric titrations is the well-defined stoichiometry with one equivalent of base or acid referring to one COOH group if completely equilibrated. Such a general transferability of binding stoichiometries among different particles is not necessarily the case for colorimetric assays.[26,78] In fact, a general one-to-one binding stoichiometry has long been assumed for the TB assay,[30−32] but comparison with other established methods were only attempted in a few exceptional cases. Surprisingly, many of these case studies revealed inconsistencies, which were mainly interpreted as a consequence of surface polymer morphology (vide infra) instead of a discrepancy in binding stoichiometry,[28,29] as proposed herein for the first time. In direct comparison, the Ni^{2+}/PV assay is faster and more user friendly, which renders it particularly useful for rapid determination of surface concentrations of COOH groups, either for qualitative purposes or, when calibrated, for routine measurements as, for example, in quality control during particle synthesis.

With regard to determining the number of accessible surface functional groups we conclude that fluorophore labeling is a practically unsuitable method for routine and accurate *quantifications*. This is a surprising and important result because of the apparently ubiquitous use of fluorophore labeling to determine surface groups and use of fluorophore-labeled biomolecules to assess their conjugation efficiency.[33,36,40−42,49,50,79] The so far reported studies disregarded the main difficulty of relating the measured fluorescence intensity to an *absolute* concentration of surface-bound fluorophores by completely neglecting the potential alteration of the molar absorption coefficient and, in particular, of the fluorescence quantum yield. As such, the measured fluorescence intensity was related to the independently determined total number of surface groups and served only as a measure for the total number of surface groups, but did not report on the number of accessible surface functional groups. Although fluorescence quenching at high surface concentrations has frequently been considered (and could be routinely avoided by the surface dilution method proposed herein),[33,42,43,49,50,80,81] our results indicate that, even in the absence of fluorophore−fluorophore interactions, an uncertainty about the fluorescence quantum yield by up to a factor of 3 will remain. This shortcoming also extends to particle-based applications in bioassays and medical diagnosis, in which relative fluorescence intensities expressed as molecules of equivalent soluble fluorophores (MESF) values are compared rather than absolute concentrations of fluorophores in different media.[67,82−84] Since MESF values are also used for determining binding kinetics and dissociation constants of ligand−receptor interactions, errors introduced by neglecting an altered fluorescence quantum yield will be carried over to fundamental biochemical parameters.[84] For quantification of functional groups on self-assembled monolayers on planar substrates, Borguet and co-workers proposed an interesting approach in which they calibrated the fluorophore concentration by evaporating a drop of a standard solution with known concentration in the area illuminated by the excitation light source.[50] This may, however, become more involved for thicker and less ordered surface structures because physical properties such as solvation and micropolarity can vary markedly within a few nanometers at interfaces,[85] and this approach is clearly not suited for particles.

Therefore, the CB7 assay represents an attractive alternative because the fluorescence detection step is performed in homogeneous solution after removal of particles by centrifu-

gation. This completely eliminates uncertainties related to a heterogeneous microenvironment, which is reflected in consistent results between the CB7 assay and the thoroughly calibrated fluorophore labeling approach. The CB7 assay also allows surface group quantifications for fluorescently encoded particles in which spectral cross-talk between fluorophores may be otherwise obstructive. Furthermore, the CB7 assay is excellently reproducible as reflected in a variation coefficient of 6%, the correlation with the number of total functional groups is even better ($R > 0.99$), and the CB7 assay requires significantly less effort, because only one modified particle is prepared instead of a series of particles with varying degrees of fluorophores, which each require additional incubation steps for protecting group removal. Moreover, covalent surface functionalization commonly requires a large excess of reactant, in particular, for COOH labeling,[52] such that the difference between reactant concentration in the supernatant before and after reaction is commonly too small to be quantified in a reliable manner.[18,26,27,33,34,86−88] In contrast, noncovalent, supramolecular complex formation between adamantylmethylamines and CB7 is reversible, quantitative, and immediate at low concentrations, such that we propose adamantylmethylamines as convenient and easy to introduce quantification tags, which complement fluorescence tags in quantifying, for example, DNA or peptides on solid supports. There is also no obvious reason why the CB7 assay should not be applicable to planar substrates, which could be dipped into a CB7 containing solution.

Accessible Functional Groups and Surface Morphology. The differentiation between the *total* and the *accessible* number of surface functional groups is generally made according to the quantification method involved, i.e., surface functional groups are considered as accessible when they can be chemically derivatized with a detection label. However, a direct comparison between total and accessible functional groups has rarely been attempted.[35] In particular, how the fraction of accessible groups varies depending on the total number of functional groups has barely been scrutinized. Previous reports noted a different chemical reactivity of surface groups compared to functional groups in homogeneous solution, which has been attributed to several factors such as steric crowding owing to the constrained environment, different solvation and micropolarity, or an altered local concentration of dissolved reagents due to preferable partitioning or limited diffusion into the surface layer.[89−91] Because all these physicochemical properties gradually change at an interface[85] and are thus dependent on the thickness of the surface layer, we expected that the fraction of accessible groups would vary with the total number of surface functional groups. However, the linear correlations between the total number of surface functional groups and the results from the fluorophore labeling approach, the CB7 assay, the TB assay, and the Ni^{2+}/PV assay clearly demonstrate that this is not the case. Accordingly, the grafted PAA presumably does not constitute a densely packed polymer shell into which diffusion of molecules smaller than CB7 would become gradually more hindered but should be rather considered as an open, porous network in which polymer chains can be addressed at their full length. In contrast, the results from biolabeling showed saturation behavior at monolayer densities, which indicates that streptavidin is too large to diffuse into this network, such that we tentatively ascribe a pore diameter that lies between the size of CB7 (ca.

1.6 nm outer diameter)[92] and streptavidin (ca. 6.5 nm diameter).[77]

On the basis of this simplified working model, the contributing factors that lead to the different ratios of total functional groups to bound probe molecules (termed stoichiometry factor n herein) can be dissected. This ratio ranges from $n = 2.65$ for Ni^{2+} binding to $n \approx 20$ for the CB7 assay.[26] For the TB assay, deviations from the stipulated one-to-one stoichiometry have been previously interpreted in terms of a dense polymer network in which TB cannot diffuse to buried COOH groups but only binds to the uppermost surface layer in a quantitative manner.[28−32] However, the clearly linear correlation between the TB assay and the conductometry values well beyond surface COOH monolayer densities suggests that diffusion of TB into the polymer network is not limited, such that the stoichiometry factor of $n = 3.4$ reflects the steric constraints on a single polymer chain (i.e., the larger size of TB compared to a COOH group) rather than a high density of polymer chains on the particle surface. The lower stoichiometry factor of $n = 2.65$ for the much smaller Ni^{2+} dication is also in line with this interpretation. The difference between the similarly sized FL-A and TB (the coupling yield of ca. 5% for FL-A refers to a stoichiometry factor of $n \approx 20$) can, however, not be rationalized by steric constraints alone and points to the intrinsic yield of the labeling reaction as an additional factor. For example, model studies on homogeneously dispersed PAA hydrogels suggested intermediate anhydride formation between adjacent COOH groups in EDC-activated coupling reactions, and just this factor alone would already limit the maximally achievable reaction yield to 50%.[53] As such, the achievable coupling yields should be explicitly considered in surface functional quantifications relying on covalent labeling. Furthermore, the fact that the larger CB7 affords a very similar stoichiometry factor suggests that the intrinsic reaction yield may even be the dominant factor in the case of covalent surface modification.

Finally, the results reported herein are directly practically relevant for determining the stoichiometry of a labeling reaction and thus assessing the amount of label required. Our results indicate that substoichiometric amounts (ca. 0.2 equiv with regard to the total number of surface COOH groups) of *N*-(adamantane methyl)-butane-1,4-diamine and FL-A/H$_2$N−CH$_2$(OCH$_2$)$_3$−CO$_2$*t*Bu are sufficient to afford the maximally achievable coupling yield, which contrasts with standard coupling protocols recommending a 1- to 10-fold molar excess.[52] Therefore, a quick determination of the maximally achievable coupling yield by, e.g., the CB7 assay would allow large amounts of precious material to be saved in particle labeling reactions.

■ CONCLUSION

We presented one of the most comprehensive comparisons of simple and readily available methods for quantification of surface functional groups. Reference values were obtained by well-established conductometric titrations and additionally validated by an innovative solid-state ^{13}C NMR approach. These values were compared to results from two colorimetric assays (TB and Ni^{2+}/PV assay), fluorophore labeling, and an assay based on supramolecular host−guest interactions (CB7 assay). Scrutiny of the fluorophore labeling approach revealed several shortcomings of this popular but frequently indiscriminately applied method. In particular, alterations of the fluorescence quantum yields should be thoroughly considered

in fluorescence-based medical diagnosis and bioassays.[67,82−84] It is quite likely that this unexpected behavior for fluorescein will also apply to other types of fluorescent dyes, such that potential changes in the fluorescence quantum yield must be explicitly considered for fluorometric quantifications. As an attractive alternative, the supramolecular CB7 assay has been established further, and adamantylmethylamines are proposed as convenient quantification tags. From the combined results, a porous and accessible surface polymer morphology was inferred, which allowed dissecting different contributions to the number of probe molecules that can be bound to the surface polymer. This also suggested that the proposed reasons leading to deviations from the postulated one-to-one binding stoichiometry of the TB assay do not hold true for the particles investigated herein.

ASSOCIATED CONTENT

Supporting Information
Experimental details and more specialized discussions. This material is available free of charge via the Internet at http://pubs.acs.org.

AUTHOR INFORMATION

Corresponding Author
E-mail: andreas.hennig@bam.de; ute.resch@bam.de
Notes
The authors declare no competing financial interest.

ACKNOWLEDGMENTS

REFERENCES

(1) Baumes, J. M.; Gassensmith, J. J.; Giblin, J.; Lee, J. J.; White, A. G.; Culligan, W. J.; Leevy, W. M.; Kuno, M.; Smith, B. D. Nat. Chem. 2010, 2, 1025−1030.
(2) Abdelrahman, A. I.; Dai, S.; Thickett, S. C.; Ornatsky, O.; Bandura, D.; Baranov, V.; Winnik, M. A. J. Am. Chem. Soc. 2009, 131, 15276−15283.
(3) Barner, L. Adv. Mater. 2009, 21, 2547−2553.
(4) Chen, J.; Hessler, J. A.; Putchakayala, K.; Panama, B. K.; Khan, D. P.; Hong, S.; Mullen, D. G.; DiMaggio, S. C.; Som, A.; Tew, G. N.; Lopatin, A. N.; Baker, J. R.; Banaszak Holl, M. M.; Orr, B. G. J. Phys. Chem. B 2009, 113, 11179−11185.
(5) Resch-Genger, U.; Grabolle, M.; Cavaliere-Jaricot, S.; Nitschke, R.; Nann, T. Nat. Methods 2008, 5, 763−775.
(6) Piao, Y.; Burns, A.; Kim, J.; Wiesner, U.; Hyeon, T. Adv. Funct. Mater. 2008, 18, 3745−3758.
(7) Kumar, R.; Roy, I.; Ohulchanskyy, T. Y.; Goswami, L. N.; Bonoiu, A. C.; Bergey, E. J.; Tramposch, K. M.; Maitra, A.; Prasad, P. N. ACS Nano 2008, 2, 449−456.
(8) De Silva, A. P.; James, M. R.; McKinney, B. O. F.; Pears, D. A.; Weir, S. M. Nat. Mater. 2006, 5, 787−790.
(9) Lu, Y.; Mei, Y.; Drechsler, M.; Ballauff, M. Angew. Chem., Int. Ed. 2006, 45, 813−816.
(10) Sharma, P.; Brown, S.; Walter, G.; Santra, S.; Moudgil, B. Adv. Colloid Interface Sci. 2006, 123−126, 471−485.
(11) Wang, L.; Wang, K.; Santra, S.; Zhao, X.; Hilliard, L. R.; Smith, J. E.; Wu, Y.; Tan, W. Anal. Chem. 2006, 78, 646−654.
(12) Jin, H. J.; Choi, H. J.; Yoon, S. H.; Myung, S. J.; Shim, S. E. Chem. Mater. 2005, 17, 4034−4037.
(13) Medintz, I. L.; Uyeda, H. T.; Goldman, E. R.; Mattoussi, H. Nat. Mater. 2005, 4, 435−446.
(14) Zhang, J. G.; Xu, S. Q.; Kumacheva, E. J. Am. Chem. Soc. 2004, 126, 7908−7914.
(15) Jal, P. K.; Patel, S.; Mishra, B. K. Talanta 2004, 62, 1005−1028.
(16) Han, M. Y.; Gao, X. H.; Su, J. Z.; Nie, S. Nat. Biotechnol. 2001, 19, 631−635.
(17) Holländer, A. Surf. Interface Anal. 2004, 36, 1023−1026.
(18) Goddard, J. M.; Hotchkiss, J. H. Prog. Polym. Sci. 2007, 32, 698−725.
(19) Gaborieau, M.; Nebhani, L.; Graf, R.; Barner, L.; Barner-Kowollik, C. Macromolecules 2010, 43, 3868−3875.
(20) Goldmann, A. S.; Walther, A.; Nebhani, L.; Joso, R.; Ernst, D.; Loos, K.; Barner-Kowollik, C.; Barner, L.; Müller, A. H. E. Macromolecules 2009, 42, 3707−3714.
(21) Okubo, M.; Suzuki, T.; Tsuda, N. Colloid Polym. Sci. 2006, 284, 1319−1323.
(22) Lorenz, O.; Breidenich, N.; Denter, U.; Reinmöller, K.-H.; Rose, G. Angew. Makromol. Chem. 1982, 103, 159−185.
(23) Suzuki, H.; Wang, B.; Yoshida, R.; Kokufuta, E. Langmuir 1999, 15, 4283−4288.
(24) Li, P.; Xu, J. J.; Wang, Q.; Wu, C. Langmuir 2000, 16, 4141−4147.
(25) Hoare, T.; Pelton, R. Langmuir 2004, 20, 2123−2133.
(26) Hennig, A.; Hoffmann, A.; Borcherding, H.; Thiele, T.; Schedler, U.; Resch-Genger, U. Anal. Chem. 2011, 83, 4970−4974.
(27) Rödiger, S.; Ruhland, M.; Schmidt, C.; Schroder, C.; Grossmann, K.; Bohm, A.; Nitschke, J.; Berger, I.; Schimke, I.; Schierack, P. Anal. Chem. 2011, 83, 3379−3385.
(28) Barish, J. A.; Goddard, J. M. J. Appl. Polym. Sci. 2011, 120, 2863−2871.
(29) Clochard, M. C.; Begue, J.; Lafon, A.; Caldemaison, D.; Bittencourt, C.; Pireaux, J. J.; Betz, N. Polymer 2004, 45, 8683−8694.
(30) Kang, E. T.; Tan, K. L.; Kato, K.; Uyama, Y.; Ikada, Y. Macromolecules 1996, 29, 6872−6879.
(31) Sano, S.; Kato, K.; Ikada, Y. Biomaterials 1993, 14, 817−822.
(32) Uchida, E.; Uyama, Y.; Ikada, Y. Langmuir 1993, 9, 1121−1124.
(33) Ivanov, V. B.; Behnisch, J.; Hollander, A.; Mehdorn, F.; Zimmermann, H. Surf. Interface Anal. 1996, 24, 257−262.
(34) Hennig, A.; Hoffmann, A.; Borcherding, H.; Thiele, T.; Schedler, U.; Resch-Genger, U. Chem. Commun. 2011, 47, 7842−7844.
(35) Graf, N.; Lippitz, A.; Gross, T.; Pippig, F.; Hollander, A.; Unger, W. E. S. Anal. Bioanal. Chem. 2010, 396, 725−738.
(36) Blanco-Canosa, J. B.; Medintz, I. L.; Farrell, D.; Mattoussi, H.; Dawson, P. E. J. Am. Chem. Soc. 2010, 132, 10027−10033.
(37) Sapsford, K. E.; Pons, T.; Medintz, I. L.; Higashiya, S.; Brunel, F. M.; Dawson, P. E.; Mattoussi, H. J. Phys. Chem. C 2007, 111, 11528−11538.
(38) Panella, B.; Vargas, A.; Ferri, D.; Baiker, A. Chem. Mater. 2009, 21, 4316−4322.
(39) Huang, S.; Joso, R.; Fuchs, A.; Barner, L.; Smith, S. V. Chem. Mater. 2008, 20, 5375−5380.
(40) Hoffmann, K.; Mix, R.; Resch-Genger, U.; Friedrich, J. F. Langmuir 2007, 23, 8411−8416.
(41) Qi, K.; Ma, Q. G.; Remsen, E. E.; Clark, C. G.; Wooley, K. L. J. Am. Chem. Soc. 2004, 126, 6599−6607.
(42) Xing, Y. J.; Dementev, N.; Borguet, E. Curr. Opin. Solid State Mat. Sci. 2007, 11, 86−91.
(43) Henneuse-Boxus, C.; De Ro, A.; Bertrand, P.; Marchand-Brynaert, J. Polymer 2000, 41, 2339−2348.
(44) Würth, C.; Lochmann, C.; Spieles, M.; Pauli, J.; Hoffmann, K.; Schuttrigkeit, T.; Franzl, T.; Resch-Genger, U. Appl. Spectrosc. 2010, 64, 733−741.
(45) Würth, C.; Grabolle, M.; Pauli, J.; Spieles, M.; Resch-Genger, U. Anal. Chem. 2011, 83, 3431−3439.
(46) Würth, C.; Pauli, J.; Lochmann, C.; Spieles, M.; Lehmann, A.; Resch-Genger, U. Anal. Chem. 2012, 84, 1345−1352.
(47) In the case of well-resolved solution spectra, integration of satellite peaks allows quantifying minor components down to 0.1%, see, for example: Claridge, T. D. W.; Davies, S. G.; Polywka, M. E. C.;

Roberts, P. M.; Russell, A. J.; Savory, E. D.; Smith, A. D. *Org. Lett.* **2008**, *10*, 5433−5436.

(48) Butterfield, S. M.; Hennig, A.; Matile, S. *Org. Biomol. Chem.* **2009**, *7*, 1784−1792.

(49) Flink, S.; van Veggel, F.; Reinhoudt, D. N. *J. Phys. Org. Chem.* **2001**, *14*, 407−415.

(50) McArthur, E. A.; Ye, T.; Cross, J. P.; Petoud, S.; Borguet, E. *J. Am. Chem. Soc.* **2004**, *126*, 2260−2261.

(51) Hoffmann, K.; Resch-Genger, U.; Mix, R.; Friedrich, J. *J. Fluoresc.* **2006**, *16*, 441−448.

(52) Hermanson, G. T.; *Bioconjugate Techniques*; 2nd ed.; Academic Press: London, 2008; pp 595−599.

(53) Nakajima, N.; Ikada, Y. *Bioconjugate Chem.* **1995**, *6*, 123−130.

(54) Park, J.; Lee, H. Y.; Cho, M. H.; Park, S. B. *Angew. Chem., Int. Ed.* **2007**, *46*, 2018−2022.

(55) McKinney, R. M.; Spillane, J. T.; Pearce, G. W. *Anal. Biochem.* **1966**, *14*, 421−428.

(56) Sun, W.-C.; Gee, K. R.; Klaubert, D. H.; Haugland, R. P. *J. Org. Chem.* **1997**, *62*, 6469−6475.

(57) Klonis, N.; Clayton, A. H. A.; Voss, E. W.; Sawyer, W. H. *Photochem. Photobiol.* **1998**, *67*, 500−510.

(58) Lamouche, G.; Lavallard, P.; Gacoin, T. *Phys. Rev. A* **1999**, *59*, 4668.

(59) Mohanty, J.; Nau, W. M. *Photochem. Photobiol. Sci.* **2004**, *3*, 1026−1031.

(60) Grabolle, M.; Brehm, R.; Pauli, J.; Dees, F. M.; Hilger, I.; Resch-Genger, U. *Bioconjugate Chem.* **2012**, *23*, 287−292.

(61) Arbeloa, I. L. *J. Chem. Soc., Faraday Trans. 2* **1981**, *77*, 1725−1733.

(62) Boyer, J.-C.; van Veggel, F. C. J. M. *Nanoscale* **2010**, *2*, 1417−1419.

(63) Huber, A.; Behnke, T.; Würth, C.; Jäger, C.; Resch-Genger, U. *Anal. Chem.* **2012**, *84*, 3654−3661.

(64) Martini, M.; Montagna, M.; Ou, M.; Tillement, O.; Roux, S.; Perriat, P. *J. Appl. Phys.* **2009**, *106*, 094304.

(65) Mirenda, M.; Lagorio, M. G.; San Román, E. *Langmuir* **2004**, *20*, 3690−3697.

(66) Tomasini, E. P.; San Román, E.; Braslavsky, S. E. *Langmuir* **2009**, *25*, 5861−5868.

(67) Finger, I.; Phillips, S.; Mobley, E.; Tucker, R.; Hess, H. *Lab Chip* **2009**, *9*, 476−478.

(68) Mineno, T.; Ueno, T.; Urano, Y.; Kojima, H.; Nagano, T. *Org. Lett.* **2006**, *8*, 5963−5966.

(69) Moghaddam, S.; Yang, C.; Rekharsky, M.; Ko, Y. H.; Kim, K.; Inoue, Y.; Gilson, M. K. *J. Am. Chem. Soc.* **2011**, *133*, 3570−3581.

(70) Ko, Y. H.; Hwang, I.; Lee, D.-W.; Kim, K. *Isr. J. Chem.* **2011**, *51*, 506−514.

(71) Nau, W. M.; Ghale, G.; Hennig, A.; Bakirci, H.; Bailey, D. M. *J. Am. Chem. Soc.* **2009**, *131*, 11558−11570.

(72) Ghale, G.; Ramalingam, V.; Urbach, A. R.; Nau, W. M. *J. Am. Chem. Soc.* **2011**, *133*, 7528−7535.

(73) Chinai, J. M.; Taylor, A. B.; Ryno, L. M.; Hargreaves, N. D.; Morris, C. A.; Hart, P. J.; Urbach, A. R. *J. Am. Chem. Soc.* **2011**, *133*, 8810−8813.

(74) Faure, A.-C.; Hoffmann, C.; Bazzi, R.; Goubard, F.; Pauthe, E.; Marquette, C. A.; Blum, L. J.; Perriat, P.; Roux, S.; Tillement, O. *ACS Nano* **2008**, *2*, 2273−2282.

(75) Wu, C.; Schneider, T.; Zeigler, M.; Yu, J.; Schiro, P. G.; Burnham, D. R.; McNeill, J. D.; Chiu, D. T. *J. Am. Chem. Soc.* **2010**, *132*, 15410−15417.

(76) Smith, P. K.; Krohn, R. I.; Hermanson, G. T.; Mallia, A. K.; Gartner, F. H.; Provenzano, M. D.; Fujimoto, E. K.; Goeke, N. M.; Olson, B. J.; Klenk, D. C. *Anal. Biochem.* **1985**, *150*, 76−85.

(77) Le Trong, I.; Wang, Z.; Hyre, D. E.; Lybrand, T. P.; Stayton, P. S.; Stenkamp, R. E. *Acta Crystallogr., Sect. D: Biol. Crystallogr.* **2011**, *67*, 813−821.

(78) Dawydoff, W.; Linow, K. J.; Philipp, B. *Acta Polym.* **1991**, *42*, 646−650.

(79) Casanova, D.; Giaume, D.; Moreau, M. l.; Martin, J.-L.; Gacoin, T.; Boilot, J.-P.; Alexandrou, A. *J. Am. Chem. Soc.* **2007**, *129*, 12592−12593.

(80) Hofstraat, J. W.; van Houwelingen, G. D. B.; van der Tol, E. B.; van Zeijl, W. J. M. *Anal. Chem.* **1994**, *66*, 4408−4415.

(81) Hofstraat, J. W.; van Houwelingen, G. D. B.; Schotman, A. H. M.; Nuijens, M. J.; Gooijer, C.; Velthorst, N. H.; Strekowski, L.; Patonay, G. *Polymer* **1997**, *38*, 4033−4041.

(82) Schwartz, A.; Wang, L.; Early, E.; Gaigalas, A.; Zhang, Y.-z.; Marti, G. E.; Vogt, R. F. *J. Res. Natl. Inst. Stand. Technol.* **2002**, *107*, 83−91.

(83) Wang, L.; Gaigalas, A. K.; Abbasi, F.; Marti, G. E.; Vogt, R. F.; Schwartz, A. *J. Res. Natl. Inst. Stand. Technol.* **2002**, *107*, 339−353.

(84) Chigaev, A.; Smagley, Y.; Zhang, Y.; Waller, A.; Haynes, M. K.; Amit, O.; Wang, W.; Larson, R. S.; Sklar, L. A. *J. Biol. Chem.* **2011**, *286*, 20375−20386.

(85) Uchiyama, S.; Iwai, K.; de Silva, A. P. *Angew. Chem., Int. Ed.* **2008**, *47*, 4667−4669.

(86) Chabane Sari, S. M.; Debouttiere, P. J.; Lamartine, R.; Vocanson, F.; Dujardin, C.; Ledoux, G.; Roux, S.; Tillement, O.; Perriat, P. *J. Mater. Chem.* **2004**, *14*, 402−407.

(87) Hook, D. J.; Vargo, T. G.; Gardella, J. A.; Litwiler, K. S.; Bright, F. V. *Langmuir* **1991**, *7*, 142−151.

(88) Yoon, T.-J.; Yu, K. N.; Kim, E.; Kim, J. S.; Kim, B. G.; Yun, S.-H.; Sohn, B.-H.; Cho, M.-H.; Lee, J.-K.; Park, S. B. *Small* **2006**, *2*, 209−215.

(89) Chechik, V.; Crooks, R. M.; Stirling, C. J. M. *Adv. Mater.* **2000**, *12*, 1161−1171.

(90) Sullivan, T. P.; Huck, W. T. S. *Eur. J. Org. Chem.* **2003**, *2003*, 17−29.

(91) Chechik, V.; Stirling, C. J. M. *Langmuir* **1997**, *13*, 6354−6356.

(92) Kim, K.; Selvapalam, N.; Ko, Y. H.; Park, K. M.; Kim, D.; Kim, J. *Chem. Soc. Rev.* **2007**, *36*, 267−279.